UDC 544.18:546.26-162:544.723:544.43 doi: 10.15407/Surface.2022.14.063

C1s CORE-LEVEL BINDING ENERGY SHIFT DEPENDENCE FROM CARBON ATOMS POSITION IN GRAPHENENANOFLAKES C_{96} AND POLYCYCLIC AROMATIC HYDROCARBON $C_{96}H_{24}$: A DFT STUDY

O.S. Karpenko, V.V. Lobanov, M.T. Kartel

Chuiko Institute of Surface Chemistry of the NAS of Ukraine,
17 General Naumov Str., Kyiv 03164, Ukraine. E-mail: karpenkooksana@ukr.net

The hexagon-shape graphene nanoflakes (GNFs) limited by zigzag edges only (with doubly and triply coordinated atoms) have unique increased reactivity. Despite the high systems symmetry (D_{6h}) the Carbon atoms in GNFs occupy non-equivalent positions. Can such physical and chemical characteristics of GNFs, which depend of the atom position in the cluster, definition? This characteristic together with the simplicity of its calculation makes it possible to predict the properties of nanoflakes obtained from GNFs by introducing single and multiatomic vacancies into them or by replacing Carbon atoms with electron withdrawing and electron donating atoms. This characteristic includes the C1s core-level binding energy shifts, the maxima of which characterize the C atoms of a certain type.

The proposed work is devoted to quantum chemical calculations of the electronic density of states (DOS) of pristine hexagon-shape GNF C_{96} (multiplicity, M=5), their saturated counterpart –polycyclic aromatic hydrocarbon(PAH) $C_{96}H_{24}$ (M=1) and their derivatives with one and two single vacancies in the ground electronic state (GES). All calculations were performed using the density functional theory (DFT) method with the involvement of the valence-split basis set 6-31G (d,p). Systems with open shells were considered using the UB3LYP exchange-correlation functional. The obtained spectra were fitted using Gaussian curve fitting program to determine the binding energy for each peak.

The Gaussian function distribution of the theoretically calculated C1s core-level binding energy shifts of GNFs testified the presence of six peaks, each of which refers to a certain type of Carbon atoms. The C1s peak with the highest binding energy (-285.57 eV) is caused by contributions from the doubly coordinated edge cyclic chain (ECC) Carbon atoms. The C1s orbitals of the central hexagon (CHex) atoms and the first cyclic chain (FCC) atoms form delocalized molecular orbitals (MOs) in different parts of the cluster.

The analogous spectrum of PAH $C_{96}H_{24}$ is slightly shifted to the region of lower binding energies and contains only two well-defined peaks. The peak with a higher binding energy (-284.36 eV) is generated by the 1s states of the CHex atoms and the atoms of the FCC, which are bounded to the CHex atoms.

The electronic DOS difference in C1s core-level spectra of GNF C_{96} (M=5) and their saturated counterpart PAH $C_{96}H_{24}$ is established due to the presence of two weakly bounded π-systems in GNF and common conjugated system in PAH.

The electronic DOS of defect-containing cluster $C_{96\text{-}1(1)}$ (M=3) (one CHex atom has been removed from the C_{96}nanoflake) is generated by the C1s core-level atoms of the second cyclic chain (SCC), which are located at the different distances from the center of the nanoflake. The peak of the lowest intensity (-284.63 eV) appears in the spectrum as a reflection of the appearance of doubly coordinated Carbon atoms surrounding the single vacancy in the $C_{96\text{-}1(1)}$ nanoflake.

The analysis of the electronic DOS of the C1s core-level spectrum of the $C_{96\text{-}2(1)}$ nanoflakeis shown, that doubly coordinated Carbon atoms, concentrated around two single vacancies, are

essentially non-equivalent. If the MO with the lowest binding energy is localized on two of them – the MO with the highest binding energy is localized on the third atoms (one around each single vacancy).

The electronic C1s core-level DOS spectrum of defect-containing molecular systems with one $C_{96-1(1)}H_{24}$ and two $C_{96-2(1)}H_{24}$ single vacancies are similar to the analogous spectrum of PAH $C_{96}H_{24}$. In the first of them – one additional maximum appears due to C1s atoms surrounding the single vacancy. In the second – there are two additional maxima, each of which is generated by C1s core-level atoms adjacent to individual vacancies.

Keywords: *hexagon-shape graphene nanoflake(GNF), polycyclic aromatic hydrocarbon (PAH), electronic density of states (DOS), C1s core-level shift, density functional theory (DFT), defect-containing nanoflake, single vacancy, Gaussian curve fitting.*

Introduction

Graphene is a two-dimensional (2D) structure composed of Carbon (C) atoms located in the nodes of a crystal lattice of the honeycomb type and connected to each other exclusively by covalent bonds.

Graphene itself, as an infinite two-dimensional system of carbon atoms, is a chemically inert substance that is not very suitable for the needs of microelectronics, due to the zero density of one-electron states at the Fermi level and the absence of a band gap. It is possible to get rid of these shortcomings in several ways, namely: making the graphene-like systems of finite size, i.e. limiting the graphene sheet with edges of a certain type; creating adjustable sets of single and multiatomic vacancies, or holes (defects) of a certain size in the graphene lattice; substituting the C atoms in the graphene lattice by electron withdrawing or electron donating hetero-atoms; violating the periodic structure; atoms and molecules adsorption on the graphene plane.

The information of the link between the C atoms position in the graphene sample and its physical and chemical properties is important when each of the listed methods or a sequence of several of them is applying. The finite graphene-like samples with zigzag edges are the most interested due to theirs increased reactivity of doubly coordinated C atoms. The creation of different types of vacancies lead to an increase the number of C atoms types.

The existence of two weakly interconnected conjugated systems in hexagon-shape graphene nanoflakes (GNFs), and a single π-system – in polycyclic aromatic hydrocarbon (PAH) with similar structure, was established in our previous works [1 – 4] using quantum chemistry study. To confirm the existence of different types of Carbon atoms in GNF compared to PAH, was decided to calculate the electronic density of states (DOS) and study the C1s core-level binding energy shifts of both structures. In the future, it is possible to predict the structure of systems with optimal reactivity to facilitate their experimental studies based on the obtained theoretical data.

All calculations were performed using the software module US GAMESS [5] by the density functional theory (DFT) method [6, 7] with exchange-correlation functional by the B3LYP [8, 9] in the 6-31 G(d,p) basis set.

The C1s core-level binding energy peaks of GNF_{96}

In [1] was shown – the size of hexagon-shape GNFs C_{96} with zigzag edges is enough to pass the properties of the larger size structures. The fig. 1 shows the curve of atomization energy ($E_{at}^{\#}$, kJ/mol) depend from the number of Carbon atoms in hexagon-shape GNFs C_6 – C_{294}. The atomization energy was calculated for the ground electronic state(GES) and refers to one C-C bond. The $E_{at}^{\#}$ decreases exponentially for first three GNFs (C_6–C_{54}) and then it linearly depends on the cluster size starting from C_{96} nanoflake. The line moving to the nanoflake C_{216} reaches a plateau. The analysis of the results of the calculation properties of GNFs C_6–C_{294} testified to their similarity and weak dependence on the number of Carbon atoms in the nanoflake. Therefore, in

the future (as typical illustrations), the data obtained for GNF C_{96}in the quintet GES (M=5) and their saturated counterpart PAH $C_{96}H_{24}$ (M=1) in the singlet GES will be considered in detail.

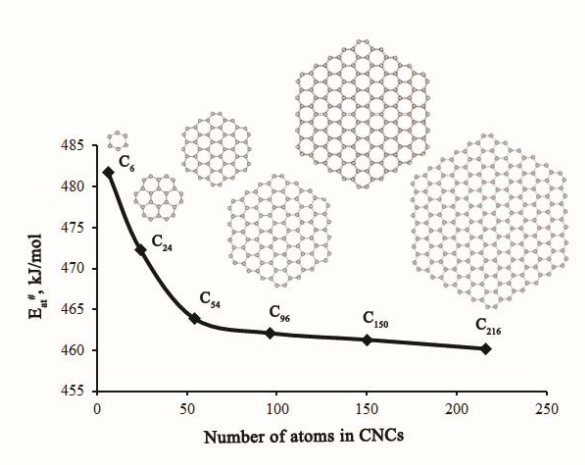

Fig. 1. Atomization energy averages over all the Carbon-Carbon bonds in GNFs C_6–C_{294} as a function of the cluster size

As known from literature [9, 10], devoted to electronic DOS calculations, the core-level binding energy shifts depend on their chemical environment in molecular system. To comparing the theoretically obtained values with experimentally measured values, the correction coefficients were introduced to compensate the quantum chemical methods errors for various types of atoms and atomic orbitals.

To reproduce the electronic DOS of GNF C_{96} (M=5) in the C1*s* core-level binding energy range, the correction coefficients of the energy scale 1.024 was used. Its value was found as the ratio of the value of 284.3 eV obtained in the experiment [9] (characteristic of the 1*s* core level of the sp^2-hybridized C atom) to 277.6 eV, which is given by the calculation of this binding energy level of the C atom in the approximation used in the work (TFG, B3LYP, 6-31G (d, p)). The same value 1.022was given in [10].

In GNFC_{96} atoms occupy several non-equivalent positions. For example, fig. 2 (which shows the atoms numbering in GNF C_{96}nanoflake) shows the edge cyclic chain (ECC) contains of three types Carbon atoms: doubly and triply coordinated and those that participate in the formation of almost triple C≡C bonds at the junctions of zigzag edges.

The non-equivalence of the Carbon atoms in the GNF is determined by the degree of hybridization of the atomic orbitals (AO), the chemical environment (the number of neighboring Carbon atoms), and possibly, their distance from the nanoflake center. The ten types of C atoms were determined in GNF C_{96} (M=5) depending on the specified factors. So there are 6 atoms of type «2», type «4» – 6, type «14» – 12, type «18» – 12, type «34» – 12, type «6» – 6, type «8» – 6, type «50» – 12, type «22» – 12 and type «38» – 12 atoms. For the C_{96} nanoflake (fig. 3), which in the experiment is identified with the photoelectron spectrum, the number of certain atoms type determines the intensity of lines in the theoretically calculated DOS spectrum in the C1*s* core-level binding energy range.

When Carbon atom is a part of a molecule or GNF, the binding energy of its 1*s*coreorbital undergoes a certain shift depending on the chemical environment of the C atom. At the same time, the C1*s* AO, in many cases, is almost 100% localized on one of the atoms, which leads to the fact that some of the lowest-energy molecular orbitals (MOs) of the nanoflake consist exclusively of the C1*s* orbital of one or another atom. So, for example, the α-MO GNF C_{96} (M=5) number one is with the lowest energy -285.86 eV (in the binding energy range with correction coefficients), the contribution of C1*s* AO with number 38 is 98% (fig. 4).

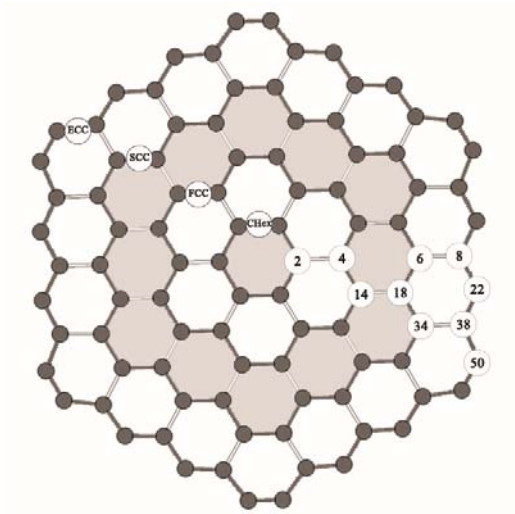

Fig. 2. Structure of GNF C_{96} nanoflake with number of main type of atoms and designation of the cyclic chains of Carbon atoms: CHex – Central Hexagon, FCC – First Cyclic Chain, SCC – Second Cyclic Chain, ECC – Edge Cyclic Chain

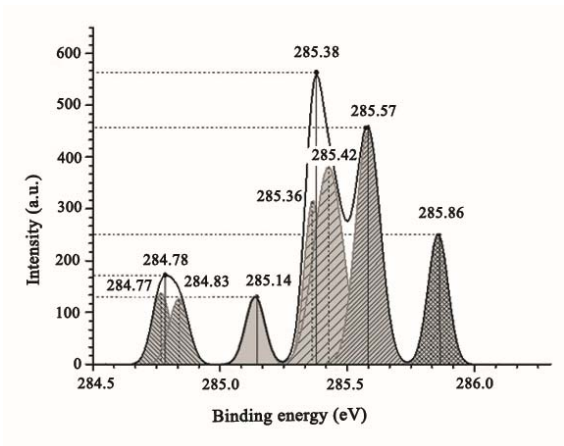

Fig. 3. C1*s* core-level DOS spectrum of GNF C_{96} (M=5) and its fitting by Gaussian functions

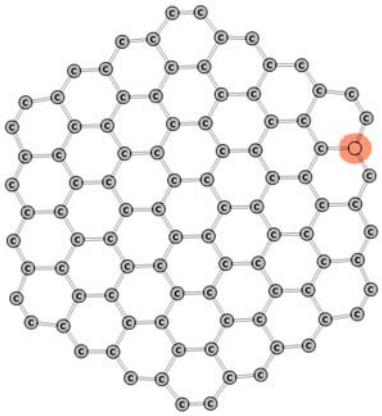

Fig. 4. Spatial localization of number one MO GNF C_{96} (M=5) in GES, which is on 98 % represented by C1*s* orbital with number 38 (numbering of atoms is shown in fig. 2)

Applying the above-described procedure for determining the energy of MOs localized on certain atoms of GNF C_{96} (M=5), the peak assignment of the theoretically calculated electronic DOS spectrum in the C1*s* core-level binding energy range was performed. Thus, the peak with an energy of -285.86 eV refers to C1*s* core-level (fig. 4) of type 38 atoms, i.e., triply coordinated C atoms of the ECC. There are 12 atoms of this type in total. The peak with a binding energy of -285.57 eV is caused by contributions from C1*s* core-level state of doubly coordinated Carbon atoms (type 22), their number is also 12. The maximum in the electronic DOS spectrum with a binding energy of -285.38 eV is formed by contributions from the local C1*s* electronic DOS of 12

carbon atoms of type 34 (binding energy -285.42 eV) and contributions from of the local C1*s* electronic DOS of 12 atoms of type 18 with an energy of -285.38 eV. The three maxima in the core-level electronic DOS spectrum of GNF C_{96} (M=5) with the lowest binding energies of -285.14, -284.83, and -284.77 eV are due to the C1*s*-electron states of types 6, 8, and 50, respectively.

Analysis of MO structure and binding energies showed that C1*s* AO of types 2, 4, and 14 form MOs that are delocalized within one or another area of the C_{96}nanoflake. In such cases, it makes no sense to assert the possibility of attributing each peaks in the electronic DOS spectrum to a specific type or types of atoms. The structure of one such nodeless delocalized MO is shown in fig. 5.

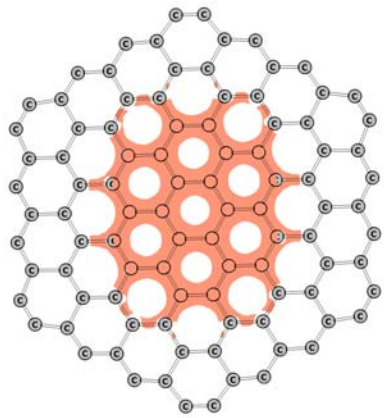

Fig. 5. Structure of the lowest-energy delocalized MO composed of AO C1*s* GNF C_{96} (M=5)

The obtained data of the C1*s* electronic DOS spectrum of C_{96} GNF (M=5) have an independent value for establishing the link between the position of the C atoms in the C_{96} nanoflake and the position of C1*s* binding energy peak. The data will be used in considering the chemical shifts in GNF with different types of vacancies in the future.

The C1s core-level binding energy peaks of PAH $C_{96}H_{24}$

The C1s core-level binding energy peaks of PAH $C_{96}H_{24}$ (Fig. 6) is somewhat shifted to the region of lower binding energies and is much simpler in comparison with the similar spectrum of GNF C_{96} (M=5). It contains two well-defined peaks (-284.36 and -284.07 eV).

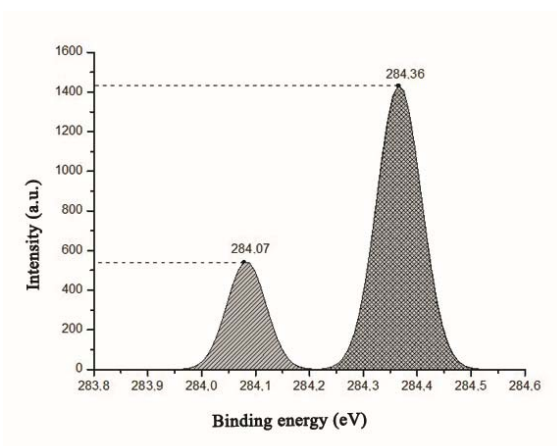

Fig. 6. DOS spectrum of PAH $C_{96}H_{24}$ in the C1*s* core-level binding energy range and its fitting by Gaussian functions

In contrast to the case of GNF C_{96} (M=5), for PAH $C_{96}H_{24}$ no MOs composed of C1*s* core-level states were detected and localized on one specific atom. As an example, in fig. 7 shows the structure of the lowest-energy MO composed of AO C1*s*, which is delocalized on a group of 12 Carbon atoms in the central part of PAH. This MO, together with MOs localized on other groups

of atoms of the central part of PAH $C_{96}H_{24}$, determine the peak with a binding energy of -284.36 eV in the 1*s* DOS spectrum. MOs distributed over the C atoms of ECC of PAH $C_{96}H_{24}$ are responsible for the peak with a binding energy of -284.07 eV (fig. 8). The difference between the 1*s* core-level electronic DOS spectra for GNF C_{96} (M=5) and PAH $C_{96}H_{24}$ is obviously caused by the presence of two weakly bounded π-systems in the first of them and one conjugated system in PAH.

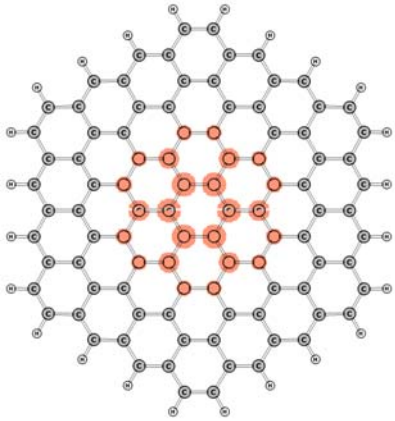

Fig. 7. Structure of the lowest-energy MO composed of C1*s* AOPAH $C_{96}H_{24}$, the electron binding energy of which corresponds to the peak at -284.36 eV in the 1s DOS spectrum

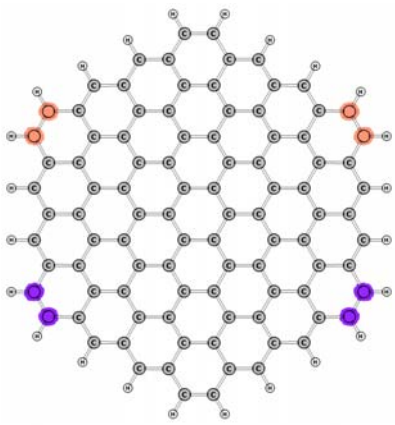

Fig. 8. Structure of one of the MOs composed of C1*s* AO PAH $C_{96}H_{24}$, the electron binding energy of which corresponds to the peak at -284.07 eV in the 1*s* DOS spectrum

The position of Carbon atoms within the nanoflake C_{96}, based on the theoretically calculated energies of C1*s* core-level spectrum, can be determined only for Carbon atoms of the ECC and SCC (see fig. 2). The localization of atoms within the FCC and the CHex cannot be established, since their 1*s*orbitals are not localized on atoms, but form delocalized MOs.

For the PAH $C_{96}H_{24}$ the C1*s* core-level DOS spectrum can distinguish only the Carbon atoms located on the periphery of the molecule from the atoms of the inner part of the molecule.

The C1s core-level binding energy peaks of defect-containing GNFs

The C1*s* core-level DOS spectrum of the defect-containing nanoflake $C_{96\text{-}1(1)}$ (M=3) (one CHex atom has been removed from the C_{96} nanoflake) is similar to the C1*s* core-level DOS spectrum of the defect-free nanoflake C_{96} (M=5) (fig. 6 and 9). As in the case of C_{96} (M=5) considered above, the peak with the highest binding energy of 1*s*-electron (-286.32 eV) refers to the most deeply placed MOs localized on the triply coordinated Carbon atoms of the ECC.

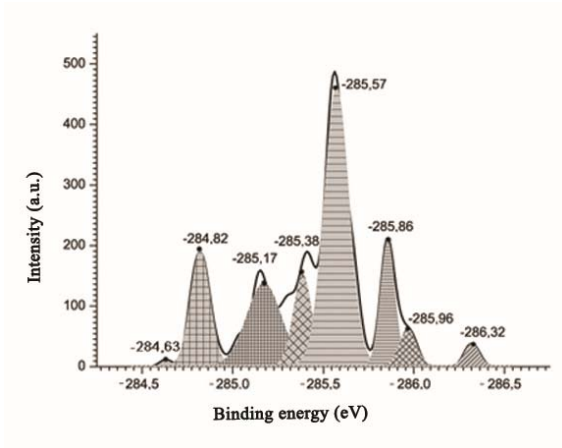

Fig. 9. C1*s* core-level DOS spectrum of nanoflake $C_{96\text{-}1(1)}$ (M=3)and its fitting by Gaussian functions

The next in binding energy (two closely spaced peaks with energies of -285.96 and -285.86 eV) are due to contributions from the C1*s* states of doubly coordinated Carbon atoms of ECC, which are in non-equivalent positions. The peak of the highest intensity (-285.57 eV) is generated by the C1*s* core-level atoms of the SCC, which are located at different distances from the center of the nanoflake. As an example, we gives atoms of types 18 and 34 (fig. 9). The peaks with lower binding energies (-285.38, -285.17 and -284.82 eV) are formed by contributions from the C1*s* core-level atoms of types 6 (SCC), 8 (triply coordinated ECC atoms located in the central part of each border) and 50 (double-coordinated Carbon atoms that take part in the formation of almost triple bonds). Finally, the peak with the lowest intensity (-284.63 eV) appears in the spectrum as a reflection of the appearance of doubly-coordinated Carbon atoms in the $C_{96\text{-}1(1)}$ nanoflake, which surround the single vacancy (fig. 9). This can be considered evidence that the properties of doubly coordinated Carbon atoms adjacent to the single vacancy differ from the properties of similar atoms of ECC. Fig. 10 shows one of the three MO localized on one of the atoms around the single vacancy. Each of the three Carbon atoms surrounding the single vacancy has a concentrated MO similar in energy and structure.

The C1*s* core-level DOS spectrum of nanoflake $C_{96\text{-}2(1)}$ (two symmetrically placed Carbon atoms of the SCC have been removed from nanoflake C_{96}) in the energy range of the C1*s* core-level (fig. 11) is somewhat more complex than the spectrum of nanoflake $C_{96\text{-}1(1)}$ with single vacancy. This is reflected both in a greater number of intensity maxima and in a significant overlap of the Gaussian functions, on which the spectrum was fitted. If for nanoflake $C_{96\text{-}1(1)}$ three degenerate MOs are localized on all three doubly coordinated Carbon atoms surrounding the vacancy, then for nanoflake $C_{96\text{-}2(1)}$ the situation is somewhat different. In particular, the MO with the lowest energy is localized on Carbon atoms concentrated around two single vacancies (fig. 12), and they correspond to the peak with a binding energy of -286.36 eV.

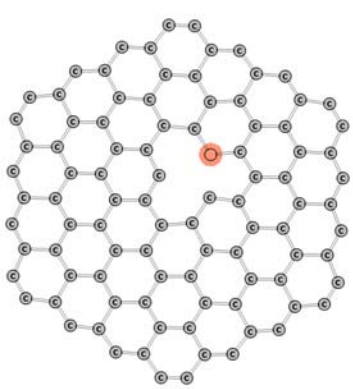

Fig. 10. Spatial localization of MO on one of the doubly coordinated Carbon atoms surrounding the single vacancy in nanoflake $C_{96\text{-}1(1)}$.

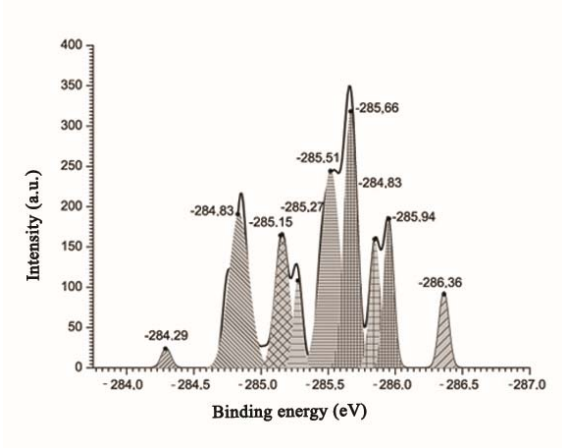

Fig. 11. C1*s* core-level DOS spectrum of nanoflake $C_{96\text{-}2(1)}$ (M=3) and its fitting by Gaussian functions

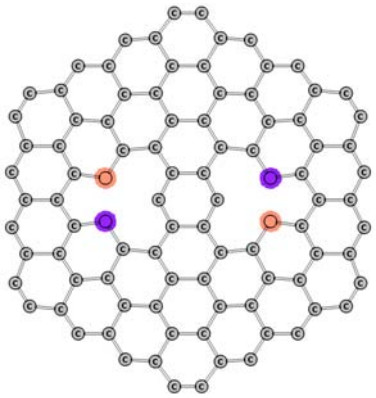

Fig. 12. Spatial localization of MO on two doubly coordinated carbon atoms surrounding single vacancies in nanoflake $C_{96\text{-}2(1)}$

In contrast to the case of nanoflake $C_{96\text{-}1(1)}$, two closely spaced peaks (-285.94 and -285.83 eV) in the C1*s* DOS spectrum of nanoflake $C_{96\text{-}2(1)}$are caused by triply coordinated atoms of the twelve-member ring of each of the single vacancies (fig. 13).

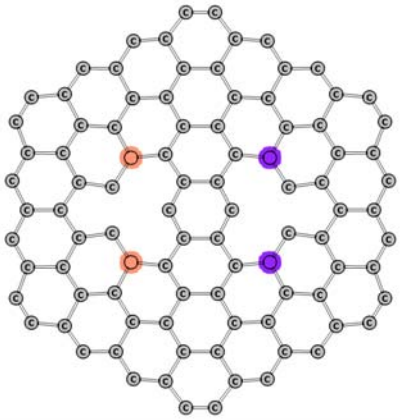

Fig. 13. The spatial localization of MO on two triply coordinated carbon atoms surrounding single vacancies in nanoflake $C_{96\text{-}2(1)}$.

The two peaks with the highest intensity (-285.66 and -285.51 eV) in the DOS spectrum of $C_{96\text{-}2(1)}$ nanoflake are caused by contributions from C1*s* of the three-fold coordinated Carbon atoms of the SCC, which is not disrupted during the formation of two single vacancies. Regarding the peaks with energies of -285.27, -285.15 and -284.83 eV, no definite conclusions can be made due to the presence of vacancies in the FCC of Carbon atoms. The peak with an energy of -284.49 eV is due to the MO concentrated on the two Carbon atoms of the CHex, which surround the single vacancy (fig. 14).

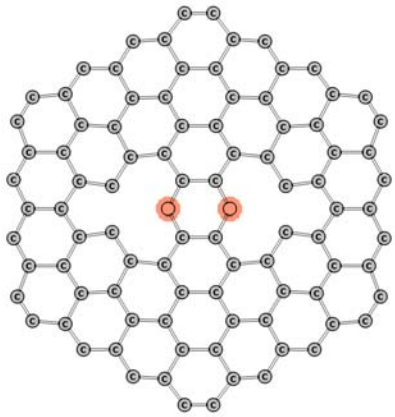

Fig. 14. Spatial localization of MO on doubly coordinated carbon atoms of the central hexagon surrounding single vacancies in nanoflake $C_{96\text{-}2(1)}$

Thus, from the analysis of the C1*s* DOS spectrum of nanoflake $C_{96\text{-}2(1)}$ it is clear that the doubly coordinated Carbon atoms, concentrated around two single vacancies, are essentially non-equivalent. If on two of them (one around each single vacancy) the MO with the lowest binding energy is localized, then on the third atoms (one around each single vacancy) – with the highest.

The C1s core-level binding energy peaks of defect-containing PAHs

It was shown above, the moving from the C_{96} nanoflake(M=5) to the PAH $C_{96}H_{24}$ the C1*s* core-level DOS spectrum is significantly simplified. A similar situation occurs when comparing the spectra of the $C_{96\text{-}1(1)}$ and $C_{96\text{-}2(1)}$ nanoflakes on the one hand and – the spectra of the $C_{96\text{-}1(1)}H_{24}$ and $C_{96\text{-}2(1)}H_{24}$ systems on the another. Fig. 15 shows the C1s core-level DOS spectrum of PAH $C_{96\text{-}1(1)}H_{24}$ (M=3). It contains two well-defined peaks of high intensity with binding energies of -284.34 and -284.09 eV and a peak of much lower intensity corresponding to an energy of -284.70 eV. This peak is generated by the C1*s* states of unsaturated atoms surrounding the single vacancy (fig. 16).

The structure of MO, the energy of which corresponds to the peak of maximum intensity -284.34 eV (fig. 17), is similar to the structure of MO PAH $C_{96}H_{24}$ (fig. 7), that is, this peak is generated by the C1*s* atoms of the central part of the system$C_{96\text{-}1(1)}H_{24}$ (M=3). The lower intensity peak with the energy of -284.09 eV is caused by the Carbon atoms of the peripheral part of the mentioned system. The spatial distribution of one of these MOs is shown in figure 18.

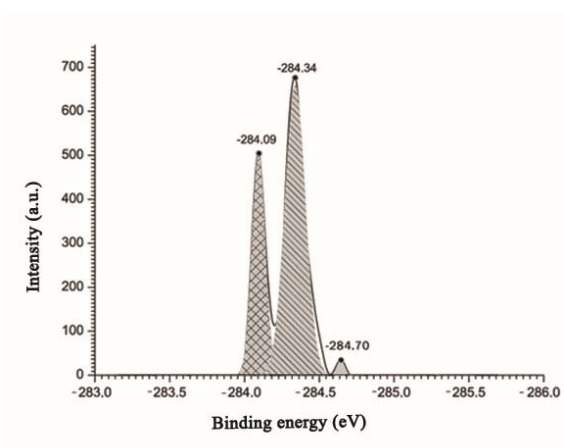

Fig. 15.C1s DOS spectrum of PAM $C_{96\text{-}1(1)}H_{24}$(M=3) and its fitting by Gaussian functions

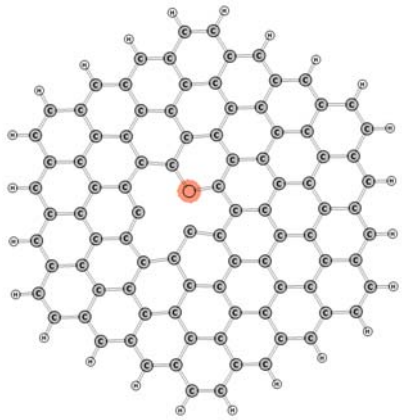

Fig. 16. Spatial localization of MO on doubly coordinated Carbon atoms surrounding a single vacancy in the $C_{96\text{-}1(1)}H_{24}$ system

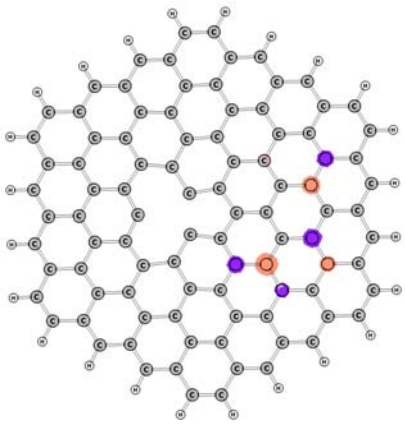

Fig. 17. Spatial localization of MOs whose energy corresponds to the maximum intensity peak of -284.34 eV in the C1*s* core-level DOS spectrum of PAH $C_{96\text{-}1(1)}H_{24}$ (M=3)

The DOS spectrum of PAM $C_{96\text{-}2(1)}H_{24}$(M=5) in the C1*s* core-level binding energy range and its fitting by Gaussian functions are shown in figure 19. It differs from the similar spectrum of $C_{96\text{-}1(1)}H_{24}$(M=3) system by the presence of one additional peak of low intensity with a binding energy of -284.78 eV. This peak refers to the C1*s* states of unsaturated C atoms that surround each of the single vacancies (fig. 20).

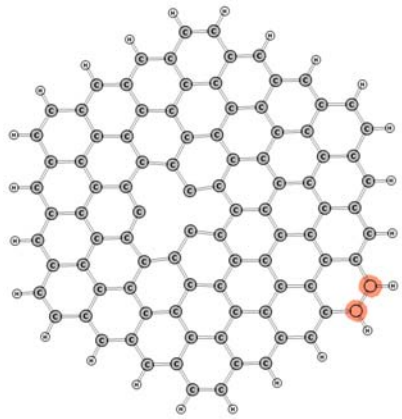

Fig. 18. Spatial localization of MOs whose energy corresponds to the peak at -284.34 eV in the C1s core-level DOS spectrum of the $C_{96\text{-}1(1)}H_{24}$ system (M=3)

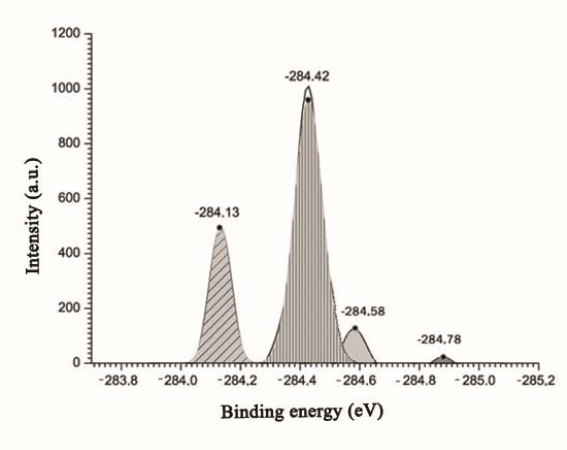

Fig. 19. Spectrum of the density of one-electron states of PAM $C_{96-2(1)}H_{24}$ (M=5) in the energy interval of the C1*s* core level and its decomposition by Gaussian functions

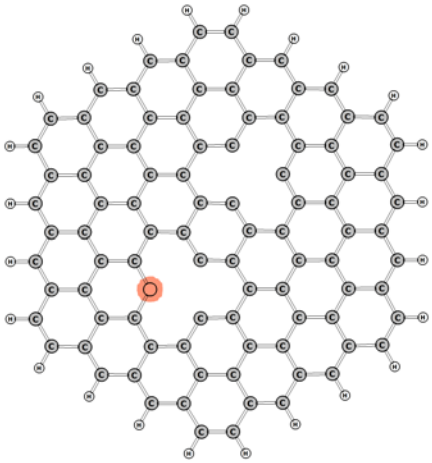

Fig. 20. Spatial localization of one of the MOs on doubly coordinated carbon atoms surrounding two single vacancies in the $C_{96-2(1)}H_{24}$ system.

The peak with a slightly lower binding energy (-284.58 eV) is generated by C1*s* states of triply coordinated Carbon atoms (fig. 21), which are located in twelve-member rings formed when two C atoms are removed from PAH C_{96}. Peaks with energies of -284.42 and -284.13 eV correspond to the MO, composed of C1*s* states of C atoms that do not border by vacancies (fig. 22), and located on the periphery of the $C_{96-2(1)}H_{24}$ system(M=5) (fig. 23).

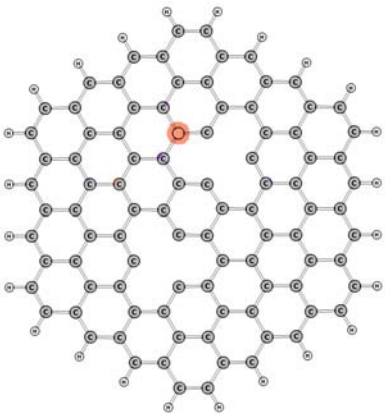

Fig. 21. Spatial localization of MOs whose energy corresponds to the peak at -284.58 eV in the spectrum of the density of one-electron states of the $C_{96-2(1)}H_{24}$system (M=5)

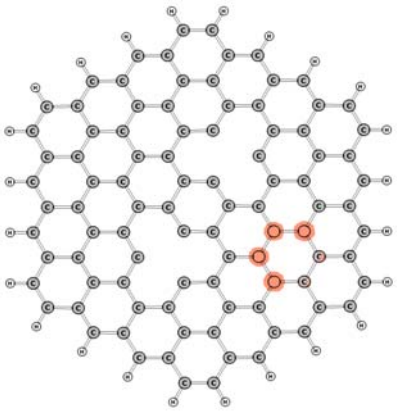

Fig. 22. Spatial localization of MOs, the energy of which corresponds to the peak of maximum intensity of -284.42 eV in the spectrum of the density of one-electron states of the $C_{96\text{-}2(1)}H_{24}$ system (M=5)

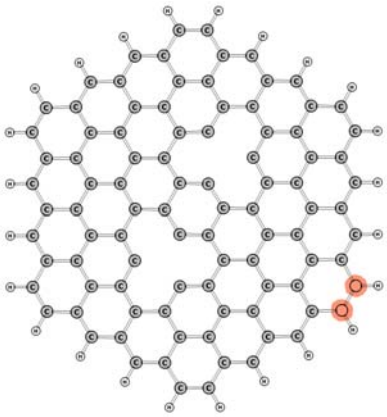

Fig. 23. Spatial localization of MOs whose energy corresponds to the peak at -284.13 eV in the spectrum of the density of one-electron states of the $C_{96\text{-}2(1)}H_{24}$ system (M=5)

Conclusions

The lowest-energy C1*s* core-level of GNF C_{96} (M=5) is localized on ECC atoms, excluding Carbon atoms, which take part in the formation of almost triple bonds at the junctions of zigzag edges. The position of Carbon atoms within the nanoflake C_{96}, based on the theoretically calculated C1*s* DOS spectrum, can be determined only for the Carbon atoms of the edge cyclic chains and second cyclic chains. The localization of atoms within the first cyclic chain and the central hexagon cannot be established, since their 1*s*orbitals are not localized on atoms, but form delocalized molecular orbitals.

For the polyaromatic molecule $C_{96}H_{24}$, the C1*s* core-level DOS spectrum in the binding energy range the can distinguish only the Carbon atoms, which are located on the periphery of the molecule, from the atoms of the inner part of the molecule. The established difference in the C1*s* core-level DOS spectra in the binding energy range for GNF C_{96} (M=5) and PAH $C_{96}H_{24}$ is obviously caused by the presence of two weakly bound π-systems in GNF and one conjugated system in PAH.

The C1*s* core-level DOS spectrum of the nanoflake$C_{96\text{-}2(1)}$ is somewhat more complex than the spectrum of the nanoflake$C_{96\text{-}1(1)}$ with a single vacancy. This is reflected both in a greater number of intensity maxima and in a significant overlap of the Gaussian functions, on which the spectrum was fitted. If for nanoflake $C_{96\text{-}1(1)}$ three degenerate MOs are localized on all three doubly coordinated Carbon atoms surrounding the single vacancy, then for nanoflake $C_{96\text{-}2(1)}$ the situation is somewhat different. In particular, the MO with the lowest energy is localized on Carbon atoms concentrated around two single vacancies, and they correspond to the peak with an energy of -286.36 eV.

The C1*s* core-level DOS spectrum of PAH $C_{96\text{-}2(1)}H_{24}$(M=5) in the binding energy range differs from the similar spectrum of the system $C_{96\text{-}1(1)}H_{24}$ (M=3) by the presence of one additional

peak with a low intensity with a binding energy of -284.78 eV. This peak refers to the C1*s* states of unsaturated Carbon atoms that surround each of the single vacancies.

The analysis of the C1*s* core-level DOS distributions of the GNF C_{96} (M=5) and PAH $C_{96}H_{24}$, as well as their defect-containing derivatives allows to identification of different types of Carbon atoms depending on the degree of hybridization of their atomic orbitals, the availability of vacancies and, to some extent, their position in the nanoflake.

References

1. Karpenko O.S., Lobanov V.V., Kartel M.T. Properties of hexagon-shaped carbon-nanoflakes. *Chem. Phys. & Tech. Surf.* 2013. **4**(2): 123. https://doi.org/10.15407/HFTP04.02.123
2. Karpenko O.S., Lobanov V.V., Kartel M.T. Structure and properties of hexagon-like carbon nanoflakes containing one and two single vacancy. *Surface*. 2013. **5**(20): 14. [in Russian] https://doi.org/10.15407/Surface
3. KarpenkoO.S., LobanovV.V., KartelM.T. Structure and properties of hexagonal graphene-like $C_{95}N$ carbonnanoflakes. *Chem. Phys. & Tech. of Surf.* 2016. **7**(2): 157. [in Russian] https://doi.org/10.15407/HFTP07.02.157.
4. Karpenko O.S., Lobanov V.V., Kartel M.T. W. Bo. Reactivity of defect-free and vacancy-containing hexagonal graphene nanoflakes according to quantum chemistry approach. *Int. J. Cur. Res. (IJCR)*. 2017. **9**(8): 55598.
5. Schmidt M.W., Baldridge K.K., Boatz J.A. *et al.* General atomic and molecular electronic structure system. *J. Comput. Chem*. 1993. **14**(11): 1347. https://doi.org/10.1002/jcc.540141112
6. Kohn W., Sham L.S. Self-consistent equation including exchange and correlation effect. *Phys. Rev. A*. 1965. **140**(4): 1133.
7. Parr R.G., Yang W. *Density-functional theory of atoms and molecules*. (Oxford: Oxford Univ. Press., 1989).
8. Becke A.D. Density-functional thermochemistry. III. The role of exchange. *J. Chem. Phys*. 1993. **98**: 5648. https://doi.org/10.1063/1.464913
9. Lee C., Yang W., Parr R.G. Development of the Colle-Salvetti correlation-energy formula into a functional of the electron density. *Phys. Rev. B*.1988. **37**(2): 785. https://doi.org/10.1103/PhysRevB.37.785
10. Yamada Y., Kim J., Matsuo S., Sato S. Nitrogen-containing graphene analyzed by X-ray photoelectron spectroscopy. *Carbon*. 2014. **70**: 59. https://doi.org/10.1016/j.carbon.2013.12.061
11. Yamada Y., Yasuda H., Murota K., Nakamura M, Sodesawa T., Sato S. Analysis of heat-treated graphite oxide by X-ray photoelectron spectroscopy. *J. Mater. Sci*. 2013. **48**: 8171. https://doi.org/10.1007/s10853-013-7630-0

Література

1. *Karpenko O.S., LobanovV.V., Kartel M.T.* Properties of hexagon-shaped carbon nanoclusters// Хімія, фізика та технологія поверхні. – 2013. – Т.4, №2. – С. 123–131.
2. *Карпенко О.С. ЛобановВ.В., КартельН.Т.* Строение и свойства углеродных нанокластеров гексагональной формы, содержащих одну и две моновакансии // Поверхность: Сб. научных тр. / Ин-т химии поверхности им. А.А. Чуйко НАН Украины; отв. ред. Н.Т. Картель. – Киев: ООО «Интерсервис», 2013. – Вып. 5(20). – С. 14–25.
3. *Карпенко О.С. Лобанов В.В., Картель Н.Т.* Строение и свойства гексагональних углеродных нанокластеров $C_{95}N$ графеноподобной структуры // Хімія, фізика та технологія поверхні. – 2016. – Т.7, №2. – С. 157–166.

4. *KartelM.T., KarpenkoO.S., LobanovV.V., BoW.* Reactivity of defect-free and vacancy-containing hexagonal graphene nanoclusters according to quantum chemistry approach // International Journal of Current Research (IJCR). – 2017. – V. 9, Iss. 8. – P. 55598–55605.
5. *Schmidt M.W., Baldridge K.K., Boatz J.A. et al.* General atomic and molecular electronic structure system // J. Comput. Chem. – 1993. – V. 14,Iss. 11. – P. 1347–1363.
6. *Kohn W., Sham L.S.* Self-consistent equation including exchange and correlation effect // Phys. Rev. A. – 1965. – V. 140, N 4. – P. 1133–1138.
7. *Parr R.G., Yang W.* Density-functional theory of atoms and molecules. – Oxford: Oxford Univ. Press, 1989. – 333 p.
8. *Becke A.D.* Density-functional thermochemistry. III. The role of exchange // J. Chem. Phys. – 1993. – V. 98. – P. 5648–5652.
9. *Lee C., Yang W., Parr R.G.* Development of the Colle-Salvetti correlation-energy formula into a functional of the electron density // Phys. Rev. B. – 1988. – V. 37, No 2. – P. 785–789.
10. *Yamada Y., Kim J., Matsuo S., Sato S.* Nitrogen-containing graphene analyzed by X-ray photoelectron spectroscopy // Carbon. – 2014. – V. 70. – P. 59–74.
11. *Yamada Y., Yasuda H., Murota K., Nakamura M,. Sodesawa T., Sato S.* An alysis of heat-treated graphit eoxide by X-ray photo electron spectroscopy // J. Mater. Sci. – 2013. – V. 48. – P. 8171–8198.

ЗАЛЕЖНІСТЬ ГУСТИНИ ОСТОВНИХ ОДНОЕЛЕКТРОННИХ СТАНІВ АТОМІВ КАРБОНУ (C1*s*) ВІД ЇХ ПОЛОЖЕННЯ У ВУГЛЕЦЕВОМУ НАНОКЛАСТЕРІ C_{96} ТА У ПОЛІАРОМАТИЧНІЙ МОЛЕКУЛІ $C_{96}H_{24}$

О.С. Карпенко, В.В. Лобанов, М.Т. Картель

Інститут хімії поверхні ім. О.О. Чуйка Національної академії наук України, вул. Генерала Наумова, 17, Київ, 03164, Україна, e-mail: karpenkooksana@ukr.net

Вуглецеві нанокластери (ВНК) гексагональної форми, обмежені тільки зигзагоподібними краями з двократно та трикратно координованими атомами Карбону, володіють підвищеною реакційною здатністю. Не дивлячись на високу симетрію (D_{6h}) таких систем, атоми Карбону в них займають нееквівалентні позиції. У зв'язку з цим постає питання щодо визначення таких їх фізико-хімічних характеристик, чисельне значення яких можна пов'язати з положенням у кластері. Наявність такої характеристики разом з простотою її обчислення дає змогу передбачити властивості нанокластерів одержаних з ВНК, введенням в них одно- та багатоатомних вакансій, або заміщенням атомів Карбону електронодонорними чи електроноакцепторними атомами. До такої характеристики відноситься спектр одноелектронних енергій, максимуми в якому однозначно характеризують атоми Карбону певного типу.

Пропонована робота присвячена квантовохімічним розрахункам спектрів одно-електронних енергій ВНК C_{96} гексагональної форми в основному квінтетному (мултиплетність, M=5) електронному стані та аналогічної за будовою поліароматичної молекули (ПАМ) $C_{96}H_{24}$, а також їх похідних з однією та двома моновакансіями. Усі розрахунки виконані методом теорії функціоналу електронної густини із залученням валентно-розщепленого базисного набору 6-31 G(d, p). Системи з відкритими оболонками розглядалися з використанням обмінно-кореляційного функціоналу UB3LYP. Одержані спектри розкладалися по набору гаусових функцій.

Розкладання по гаусовим функціям теоретично розрахованого спектра одно-електронних станів в області енергії остовного рівня C1s засвідчив про наявність шести піків, кожен з яких можна віднести до певного типу атомів Карбону. Пік з найвищою енергією зв'язування (-285.57 еВ) зумовлений внесками від C1s остовного стану двократно координованих атомів Карбону крайового циклічного ланцюжка. C1s орбіталі атомів центрального гексагона (ЦГ) та I циклічного ланцюжка утворюють делокалізовані в різних ділянках кластера молекулярні орбіталі (МО).

Аналогічний спектр ПАМ $C_{96}H_{24}$ дещо зсунутий в область нижчих енергій зв'язування остовного C1s-електрона і містить лише два чітко визначених піки. Пік з вищою енергією зв'язування (-284.36 еВ) породжується 1s-станами атомів ЦГ та атомами I циклічного ланцюжка, які зв'язані з атомами ЦГ.

Встановлена відмінність у спектрах густини одно-електронних станів в інтервалі енергії остовного рівня C1s для ВНК C_{96} (M=5) та ПАМ $C_{96}H_{24}$, очевидно, обумовлена наявністю двох слабко зв'язаних π-систем в першому з них та однієї кон'югованої системи в ПАМ.

Спектр густини одно-електронних станів дефектвмісного кластера $C_{96\text{-}1(1)}$ (M=3) (з кластера C_{96} видалено один атом ЦГ) породжується станом C1s атомів Карбону II циклічного ланцюга, які розміщуються на різних відстанях від центру кластера. Пік найнижчої інтенсивності (-284.63 еВ) виникає у спектрі як відображення появи у кластері $C_{96\text{-}1(1)}$ двократно координованих атомів Карбону, які оточують моно вакансію.

Із аналізу спектра густини одноелектронних станів кластера $C_{96\text{-}2(1)}$ в інтервалі енергії остовного рівня C1s видно, що двократно координовані атоми Карбону, зосереджені навколо двох моновакансій, суттєво нееквівалентні. Якщо на двох з них локалізована МО з найнижчою енергією зв'язування, то на третіх атомах, по одному навколо кожної моновакансії, – з найвищою.

Спектр одноелектронних станів дефектвмісних молекулярних систем з однією $C_{96\text{-}1(1)}H_{24}$ та двома $C_{96\text{-}2(1)}H_{24}$моновакансіями подібні до аналогічного спектра ПАМ $C_{96}H_{24}$. В першому з них з'являється один додатковій максимум, обумовлений C1s атомів, які оточують моновакансію. В другому спектрі присутні два додаткових максимуми, кожен з яких породжується остовними C1s станами атомів, сусідніх з індивідуальними вакансіями.

Ключові слова: *графеноподібні нанокластери гексагональної форми, поліциклічний ароматичний вуглеводень, густина електронних станів, зсув C1s остовного рівня, теорія функціоналу густини, дефектвмісний нанокластер, моновакансія, гаусова апроксимація*